Development of a consistent dynamic procedure for modeling subfilter variance

By G. Balarac, V. Raman† AND H. Pitsch

1. Motivation and objectives

Large-eddy simulation (LES) is based on the separation of turbulence scales into resolvable large scales and modeled small scales. A filtering operation,

$$\bar{f}(\mathbf{x}) = \int f(\mathbf{y}, t)\Phi(\mathbf{x} - \mathbf{y})d\mathbf{y}, \tag{1.1}$$

is used to obtain the large-scale resolved field, where $\bar{f}$ is the filtered field corresponding to a turbulent field f, and Φ the filter kernel. LES has been very successful in predicting free-shear flows, since these flows are typically controlled by large-scale energy-containing motions (Rogallo & Moin 1984; Lesieur & Métais 1996; Meneveau & Katz 1996). Several models for the subfilter unresolved terms have been proposed in this context (Pope 2000). While the LES formulation is useful in such flows, combustion or wall-bounded flows are controlled by the small-scale evolution of the turbulence, and are not naturally described by the large scales. Consequently, detailed subfilter modeling in combustion is critical in ensuring predictive accuracy. Interestingly, the ability of LES to describe large-scale scalar mixing provides a natural starting point for modeling turbulence-chemistry interactions at the small scales. In this context, the purpose of this brief is to assess the predictive accuracy of currently used models and provide improved formulations.

LES of turbulent combustion often employs conserved scalar-based formulations (Pitsch 2006). The mixture-fraction, z, is a conserved scalar that is used to describe the local thermochemical state of the fluid. To obtain the filtered thermochemical vector, the subfilter distribution of mixture-fraction is required. Since LES resolves only the large scales, this information needs to be provided through a statistical description of the subfilter state. Typically, a presumed probability density function (PDF) in the form of a beta function is used (Cook & Riley 1994). The PDF is parameterized by the filtered mixture-fraction, $\overline{z}$, and the mixture-fraction variance, $z_v = \overline{zz} - \bar{z}\bar{z}$. Since the subfilter variance is not directly available in LES, several models have been proposed for this quantity. The performance of these models is often not of satisfactory accuracy given their importance for predicting the heat release and the effect of the heat release on the large-scale motion of the flow.

In this work, we first study the performance of the most commonly used models, namely the scale-similarity model (Cook & Riley 1994) and the dynamic Smagorinsky-type model (Pierce & Moin 1998). The validity of the assumptions used to construct the dynamic Smagorinsky-type model are tested. To improve the predictive accuracy, a new dynamic procedure based on a Taylor series expansion is then proposed. The new model is then examined in *a priori* tests, and compared with the dynamic Smagorinsky-type model.

† Current Address: The University of Texas at Austin, Austin, Texas-78712 USA

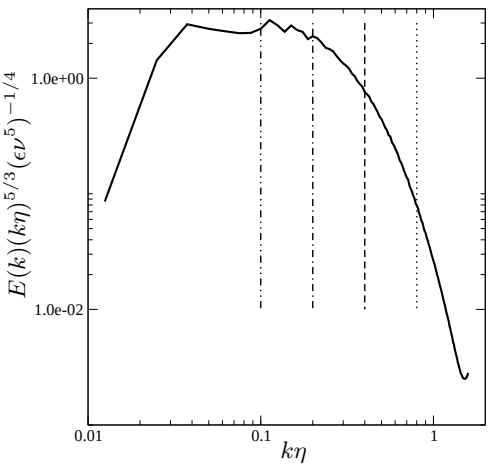

FIGURE 1. Compensated kinetic energy spectrum with the location of filters used in this work. $\Delta/\Delta x = 2$ ····· ; $\Delta/\Delta x = 4$ – – – – ; $\Delta/\Delta x = 8$ —·— ; $\Delta/\Delta x = 16$ —··— .

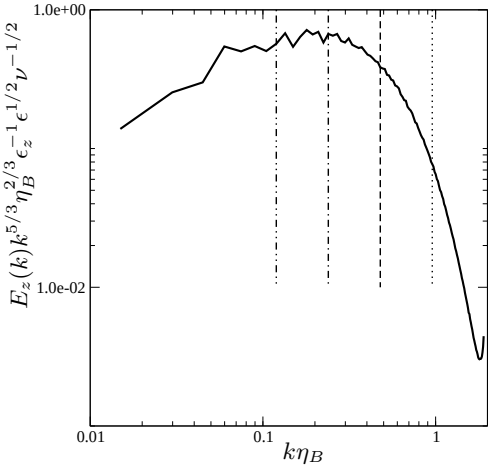

FIGURE 2. Compensated scalar variance spectrum with the location of filters used in this work (see Fig. 1 for legend).

2. Numerical method

In this work, *a priori* tests are conducted using direct numerical simulation (DNS) data from a forced homogeneous isotropic turbulence computation. A pseudo-spectral code with second-order explicit Runge-Kutta time-advancement is used. The viscous terms are treated exactly. The simulation domain is discretized using 256^3 grid points on a domain of length 2π. A classic 3/2 rule is used for dealiasing the non-linear convection term, and statistical stationarity is achieved using a forcing term (Alvelius 1999). The mixture-fraction equation is advanced simultaneously using an identical numerical scheme. To enforce stationarity of the scalar field, a mean scalar gradient is imposed (Donzis *et al.* 2005). The size of the computational domain is larger than four times the integral length scale to ensure that the largest flow structures are not affected. The simulation parameters are chosen such that $k_{max}\eta > 1.5$ and $k_{max}\eta_B > 1.5$, where k_{max} is the maximum wavenumber in the domain, and η and η_B are the Kolmogorov and Batchelor scales, respectively. The Reynolds number based on the Taylor micro-scale is approximately 100 and the molecular Schmidt number is set to 0.7. The numerical implementation has been verified by comparing the skewness and flatness of the velocity derivative with Jimenez & Wray (1998) for similar Reynolds numbers.

In the *a priori* tests, the box filter is used to replicate the behavior of the filter implicitly associated with the discretization using centered finite differences often used in LES of engineering flows (Rogallo & Moin 1984). The location in wavenumber space of the filters used are displayed in Figs. 1 and 2, which show the kinetic energy and scalar variance spectra.

3. Results

3.1. *Subfilter scalar variance models*

Several models for the subfilter variance have been proposed in the past (Cook & Riley 1994; Pierce & Moin 1998). The scale-similarity model (Cook & Riley 1994) uses the self-similar behavior of turbulent properties at different length scales to model the

subfilter variance. The scalar variance is then written as

$$z_{v,SS} = C_s \left(\widetilde{\bar{z}\bar{z}} - \tilde{\bar{z}}\tilde{\bar{z}} \right). \tag{3.1}$$

In this equation, $\tilde{\cdot}$ denotes a test filter and C_s is the scale-similarity constant that needs to be specified. C_s is highly flow dependent and is not a universal constant. Hence, *a priori* specification almost always introduces large errors (Wall *et al.* 2000). Pierce & Moin (1998) proposed a dynamic formulation based on a mixing length hypothesis similar to the Smagorinsky model. In this approach, the model constant is evaluated as a varying parameter using the filtered fields available in LES. A scalar-gradient based scaling law is used to obtain a closed-form algebraic equation for the subfilter variance

$$z_{v,DM} = C_d \Delta^2 \frac{\partial \bar{z}}{\partial x_i} \frac{\partial \bar{z}}{\partial x_i}, \tag{3.2}$$

where Δ is the filter width and C_d is the model constant that is determined dynamically. Assuming that the model coefficient varies slowly in space and that the same coefficient applies at both filter levels, Eq. 3.2 can be filtered at the filter level leading to

$$\widetilde{\bar{z}\bar{z}} - \tilde{\bar{z}}\tilde{\bar{z}} = C_d \Delta^2 \widetilde{\frac{\partial \bar{z}}{\partial x_i}} \frac{\partial \bar{z}}{\partial x_i} \tag{3.3}$$

or it can be written at the test filter level, which gives

$$\widetilde{\bar{z}\bar{z}} - \tilde{\bar{z}}\tilde{\bar{z}} = C_d \tilde{\Delta}^2 \frac{\partial \tilde{\bar{z}}}{\partial x_i} \frac{\partial \tilde{\bar{z}}}{\partial x_i}, \tag{3.4}$$

where $\tilde{\Delta}$ is the test filter width. Subtracting Eq. 3.3 from Eq. 3.4 then provides

$$L_d = C_d M_d \text{ with } L_d = \widetilde{\bar{z}\bar{z}} - \tilde{\bar{z}}\tilde{\bar{z}} \text{ and } M_d = \tilde{\Delta}^2 \frac{\partial \tilde{\bar{z}}}{\partial x_i} \frac{\partial \tilde{\bar{z}}}{\partial x_i} - \Delta^2 \widetilde{\frac{\partial \bar{z}}{\partial x_i}} \frac{\partial \bar{z}}{\partial x_i}. \tag{3.5}$$

Assuming that the coefficient is constant over homogeneous directions, C_d is then obtained using a least-squares averaging procedure

$$C_d = \frac{\langle L_d M_d \rangle}{\langle M_d M_d \rangle}, \tag{3.6}$$

where the brackets indicate averaging over homogeneous directions. Note that in the case of homogeneous turbulence, C_d is constant in all the domain.

As a first step toward understanding modeling errors, both these models were evaluated *a priori* using DNS data. For these tests, the scale similarity constant was taken to be equal to unity (Cook & Riley 1994). The models are compared using the notion of an optimal estimator (Moreau *et al.* 2006). Based on this idea, if a quantity z_v is modeled with a finite set of variables ϕ, an exact model cannot be guaranteed. If the exact solution z_v is known, for example from DNS, the optimal estimator of z_v in terms of the set of variables ϕ is given by the expectation of the quantity z_v conditioned on the variables in the set. A quadratic error can consequently be defined as the averaging of the square of the difference at each point between the conditional mean value given by the value of ϕ at this point and the exact value of the quantity,

$$\epsilon_{min} = \langle (z_v - \langle z_v | \phi \rangle)^2 \rangle, \tag{3.7}$$

where ϵ_{min} is the quadratic error, and the angular brackets indicate statistical averaging over a suitable ensemble. It should be noted that any model formulated using the variable

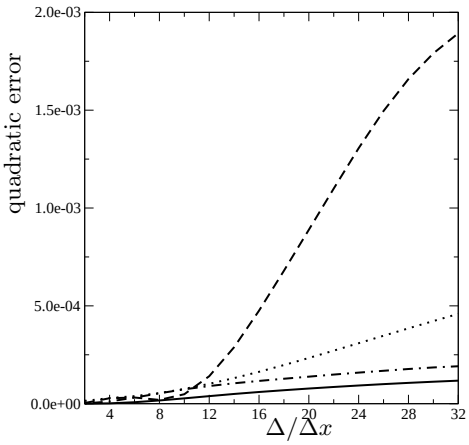

FIGURE 3. Evolution of the quadratic errors of the scale similarity and dynamic Smagorinsky–type models and their associated irreducible error with the filter width. $\langle (z_v - \langle z_v|\phi_1\rangle)^2\rangle$ ——— ; $\langle (z_v - z_{v,DM})^2\rangle$ - - - - ; $\langle (z_v - \langle z_v|\phi_2\rangle)^2\rangle$ —·— ; $\langle (z_v - z_{v,SS})^2\rangle$ ····· .

set ϕ will introduce an error that is larger than or equal to this minimum error, with the best model formulation producing this minimum error. Consequently, this quadratic error is referred to as the irreducible error. Only a change in the variable set may reduce the magnitude of this error.

For the dynamic Smagorinsky-type model, the variable set used is $\phi_1 = \left\{\frac{\partial \bar{z}}{\partial x_i}\frac{\partial \bar{z}}{\partial x_i}\right\}$, whereas the variable set for the scale-similarity model is $\phi_2 = \left\{\widetilde{\bar{z}\bar{z}} - \tilde{\bar{z}}\tilde{\bar{z}}\right\}$. Note that the variables used to define C_d in the dynamic formulation are not taken into account, since C_d is constant due to the averaging process. Figure 3 shows the quadratic errors of the scale-similarity and dynamic Smagorinsky-type models as a function of the filter width. The irreducible errors associated with the corresponding variable sets are also shown. Both models are close to the irreducible error if the filter is in the dissipation range ($\Delta/\Delta x < 8$). When the filter is located in the inertial-convective range of the scalar spectrum, the quadratic errors of each model become significantly larger than their associated irreducible errors. This is particularly true for the dynamic Smagorinsky-type model showing a very large error compared with the irreducible error for large filter size. If only the irreducible errors are compared, it is noticed that the irreducible error corresponding to the dynamic Smagorinsky-type model is always lower than the irreducible error corresponding to the scale-similarity model. These results show that a better model can potentially be formulated with the variable set ϕ_1 than for variable set ϕ_2, but that a substantial improvement is needed to achieve this goal.

While the dynamic Smagorinsky-type model produces a large quadratic error, the variable set corresponding to this model produces a relatively small irreducible error. This means that the assumptions that lead to the functional form of the model formulation introduce the errors observed in the *a priori* tests. To understand the source of these errors, the main assumptions that lead to the dynamic formulation are studied next. From Eqs. 3.2 - 3.5, the quantities C_1, C_2, C_3 and C_4 are defined from the DNS data as

$$\overline{z\bar{z}} - \bar{z}\bar{z} = C_1\Delta^2 \frac{\partial \bar{z}}{\partial x_i}\frac{\partial \bar{z}}{\partial x_i}, \tag{3.8}$$

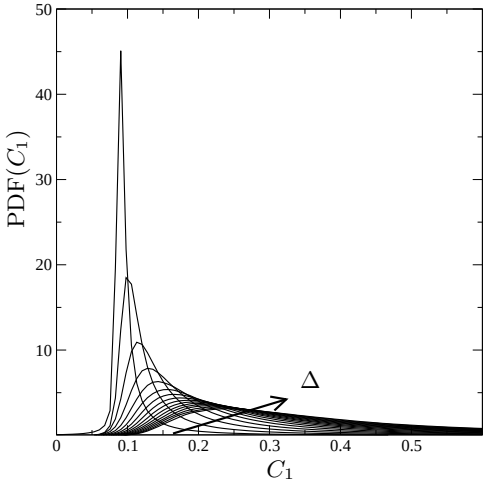

FIGURE 4. PDF of C_1 (Eq. 3.8) for several filter sizes. The arrow indicates the filter size increasing.

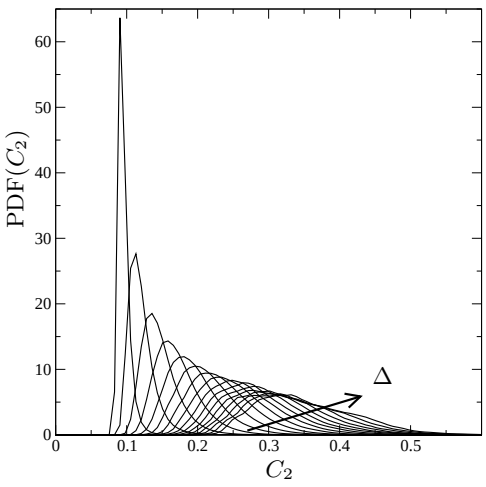

FIGURE 5. PDF of C_2 (Eq. 3.9) for several filter sizes. The arrow indicates the filter size increasing.

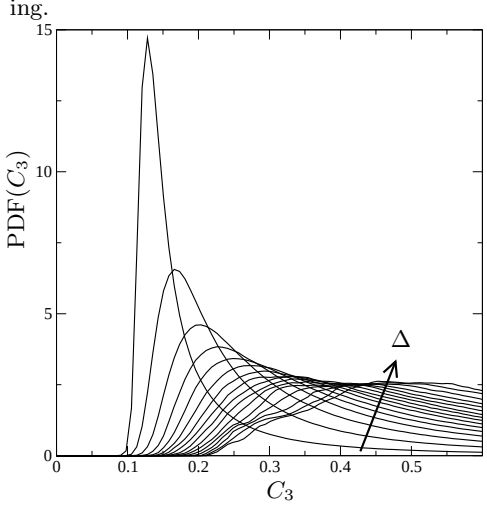

FIGURE 6. PDF of C_3 (Eq. 3.10) for several filter sizes. The arrow indicates the filter size increasing.

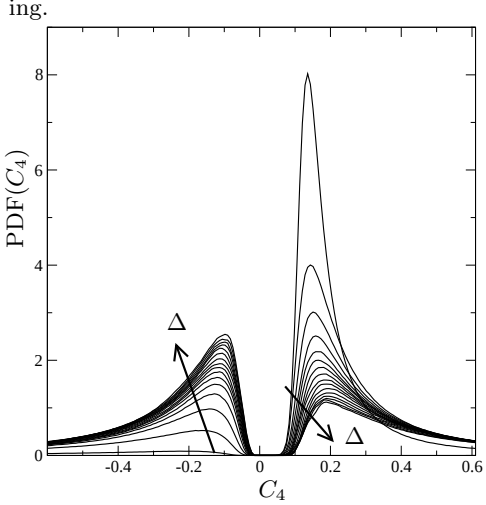

FIGURE 7. PDF of C_4 (Eq. 3.11) for several filter sizes. The arrow indicates the filter size increasing.

$$\widetilde{\overline{z}\overline{z}} - \widetilde{\overline{z}}\widetilde{\overline{z}} = C_2 \Delta^2 \frac{\partial \widetilde{\overline{z}}}{\partial x_i} \frac{\partial \overline{z}}{\partial x_i}, \tag{3.9}$$

$$\widetilde{\overline{z}\overline{z}} - \tilde{\bar{z}}\tilde{\bar{z}} = C_3 \tilde{\Delta}^2 \frac{\partial \tilde{\bar{z}}}{\partial x_i} \frac{\partial \tilde{\bar{z}}}{\partial x_i}, \text{ and} \tag{3.10}$$

$$\widetilde{\overline{z}\overline{z}} - \tilde{\bar{z}}\tilde{\bar{z}} = C_4 \left(\tilde{\Delta}^2 \frac{\partial \tilde{\bar{z}}}{\partial x_i} \frac{\partial \tilde{\bar{z}}}{\partial x_i} - \Delta^2 \frac{\partial \widetilde{\overline{z}}}{\partial x_i} \frac{\partial \overline{z}}{\partial x_i} \right). \tag{3.11}$$

Note that these quantities are spatially varying. The main modeling hypothesis of the dynamic Smagorinsky-type model is to assume that C_1, C_2 and C_3 are constant over homogeneous directions and equal to C_d. This assumption also requires C_4 to be constant over homogeneous directions and to be equal to C_d. Figures 4, 5 and 6 show the PDFs of

C_1, C_2 and C_3 for several filter sizes. The coefficients C_1 and C_2 have clearly uni-modal distributions with distinct peaks, in particular for small filter sizes. This validates the assumption of constant quantities. The distribution of C_1 shows that the model 3.2 is valid but also that the model coefficient is far from universal, even in such simple flows, and a dynamic procedure is required to improve predictive accuracy. The coefficient C_3, however, has a broad distribution even for small filter sizes showing that a constant value of C_3 cannot be assumed. Moreover, the ranges of values of C_1, C_2 and C_3 are clearly different. The assumption $C_1 = C_2 = C_3 = C_d$ is thus not verified. In this case, the equality $C_4 = C_d$ used to compute the dynamic constant cannot be true. Indeed, C_4 clearly has a bi-modal distribution and cannot be assumed to be constant (see Fig. 7). Note that C_4 contains a large negative range that would lead to negative, and hence unrealizable, variance. Both the unphysical behavior and the scale dependence of the model coefficients need to be addressed. In this context, a new model formulation is discussed next.

3.2. *Subfilter scalar variance modeling based on Taylor series*

The starting point for a new subfilter scalar variance model is based on a Taylor series expansion. This approach has already been used by several authors (Clark *et al.* 1979; Liu *et al.* 1994) to derive the so-called Clark's gradient model. Here, we briefly describe the method proposed by Bedford & Yeo (1993) to give an expansion for $\overline{fg}$ as a function of $\bar{f}$ and $\bar{g}$ and their derivatives (where f and g are quantities describing flow fields).

3.2.1. *Bedford and Yeo's expansion*

Bedford & Yeo (1993) proposed an expansion of $\overline{fg}$ based on Taylor series in the case of a Gaussian filter. The starting point is that in spectral space, the filtering operation 1.1 is

$$\widehat{\bar{f}}(\vec{k}) = \hat{f}(\vec{k})\hat{\Phi}(\vec{k}), \tag{3.12}$$

where $\hat{f}(\vec{k})$ is the Fourier transform of $f(\vec{x})$ and $\vec{k}$ is the wave vector. The Taylor series of a Gaussian filter of the form $\hat{\Phi}(\vec{k}) = \exp\left(-\Delta^2 k^2/24\right)$, is given as

$$\hat{\Phi}(\vec{k}) = 1 - \frac{\Delta^2}{24}k^2 + \frac{\Delta^4}{1152}k^4 - \frac{\Delta^6}{82944}k^6 + \dots \,. \tag{3.13}$$

Since the Laplacian operator in spectral space, $\hat{L}$, is given by

$$\hat{L}(f) = \widehat{\frac{\partial^2 f}{\partial x_i^2}} = -k^2\hat{f}(\vec{k}), \tag{3.14}$$

the inverse Fourier transform of Eq. 3.12 combined with Eq. 3.13 yields for the filtered function in physical space

$$\bar{f} = f + \frac{\Delta^2}{24}L(f) + \frac{\Delta^4}{1152}L^{(2)}(f) + \frac{\Delta^6}{82944}L^{(3)}(f) + \dots \,. \tag{3.15}$$

Moreover, in spectral space, we can write the filtering operation as

$$\hat{f}(\vec{k}) = \frac{1}{\hat{\Phi}(\vec{k})}\hat{\bar{f}}(\vec{k}). \tag{3.16}$$

We can then write a Taylor series for $1/\hat{\Phi}(\vec{k}) = \exp\left(\Delta^2 k^2/24\right)$ as

$$1/\hat{\Phi}(\vec{k}) = 1 + \frac{\Delta^2}{24}k^2 + \frac{\Delta^4}{1152}k^4 + \frac{\Delta^6}{82944}k^6 + \dots \,, \tag{3.17}$$

which leads to

$$f = \bar{f} - \frac{\Delta^2}{24}L(\bar{f}) + \frac{\Delta^4}{1152}L^{(2)}(\bar{f}) - \frac{\Delta^6}{82944}L^{(3)}(\bar{f}) + \dots \,. \tag{3.18}$$

Considering the expansion 3.15 for $\overline{fg}$, after substitution of f and g by their expansion 3.18, and after considerable algebra, Bedford & Yeo (1993) found the expansion

$$\overline{fg} = \bar{f}\bar{g} + \frac{\Delta^2}{12}\frac{\partial \bar{f}}{\partial x_i}\frac{\partial \bar{g}}{\partial x_i} + \frac{\Delta^4}{288}\frac{\partial^2 \bar{f}}{\partial x_i \partial x_j}\frac{\partial^2 \bar{g}}{\partial x_i \partial x_j} + \frac{\Delta^6}{10368}\frac{\partial^3 \bar{f}}{\partial x_i \partial x_j \partial x_k}\frac{\partial^3 \bar{g}}{\partial x_i \partial x_j \partial x_k} + \dots \,. \tag{3.19}$$

Note that this expansion is based on the Gaussian filter, and is not valid for other filters. Similar results have been derived elsewhere for the subfilter kinetic energy (Pomraning & Rutland 2002). Moreover, if $f = u_i$ and $g = u_j$, and if only the first two terms of the right-hand side (RHS) are considered, the gradient model proposed by Clark *et al.* (1979) to model the subfilter stress tensor is obtained. The Clark's relation can be used to model different types of subfilter terms as long as the modeled terms have most of their energy at large scales; otherwise, the truncation error of the expansion will be too large. For instance, da Silva & Pereira (2007) have recently modeled successfully the subfilter pressure-velocity term in the transport equation of the subfilter kinetic energy using this relation.

3.2.2. *Subfilter scalar variance modeling: new dynamic procedure*

Before deriving a new dynamic procedure, the dynamic Smagorinsky-type model assumptions can be examined in the light of expansion 3.19. We will start by deriving Eq. 3.4 from Eq. 3.19, which is the Smagorinsky-type model at the test filter scale. Note that in the derivation of the dynamic model, it is assumed that test-filtered quantities, such as $\tilde{\bar{z}}$, are obtained by first applying the filter on the regular scale and then applying the filter on the test-filter scale. Because of this, the modeling assumption used for Eq. 3.4 is not the same as that in Eq. 3.2. In fact, Eq. 3.2 follows from the mixing length assumption, whereas the model used in Eq. 3.4 would actually be the mixing length expression for $\widetilde{\bar{z}\bar{z}} - \tilde{\bar{z}}\tilde{\bar{z}}$. Using the expression 3.19 to expand $\widetilde{\bar{z}\bar{z}}$ leads to

$$\widetilde{\bar{z}\bar{z}} = \widetilde{\bar{z}}\widetilde{\bar{z}} + \frac{\Delta^2}{12}\widetilde{\frac{\partial \bar{z}}{\partial x_i}}\frac{\partial \bar{z}}{\partial x_i} + \dots = \tilde{\bar{z}}\tilde{\bar{z}} + \frac{\tilde{\Delta}^2}{12}\frac{\partial \tilde{\bar{z}}}{\partial x_i}\frac{\partial \tilde{\bar{z}}}{\partial x_i} + \frac{\Delta^2}{12}\widetilde{\frac{\partial \bar{z}}{\partial x_i}}\frac{\partial \bar{z}}{\partial x_i} + \dots \,. \tag{3.20}$$

Equation 3.20 shows that $\widetilde{\bar{z}\bar{z}} - \tilde{\bar{z}}\tilde{\bar{z}}$ cannot be described by the term $\tilde{\Delta}^2 \frac{\partial \tilde{\bar{z}}}{\partial x_i}\frac{\partial \tilde{\bar{z}}}{\partial x_i}$ without taking the term $\Delta^2 \widetilde{\frac{\partial \bar{z}}{\partial x_i}}\frac{\partial \bar{z}}{\partial x_i}$ into account. This shows that the assumption 3.4 is incorrect as previously discussed and seen in the behavior of C_3. From this follows that Eq. 3.5, which is deduced from Eq. 3.4, cannot be used for the formulation of the dynamic procedure as already seen in the behavior of C_4.

For the subfilter scalar variance, the first order of the expansion 3.19 leads to the model

$$z_{v,o2} = \frac{\Delta^2}{12}\frac{\partial \bar{z}}{\partial x_i}\frac{\partial \bar{z}}{\partial x_i}, \tag{3.21}$$

which is similar to the dynamic Smagorinsky-type model, but using $C_d = 1/12$ instead of computing C_d dynamically. One could use this constant value to compute the variance. However, since the higher-order terms of the expansion are discarded in this model, a dynamic coefficient, C_n, can be introduced to account for the truncation error. The new

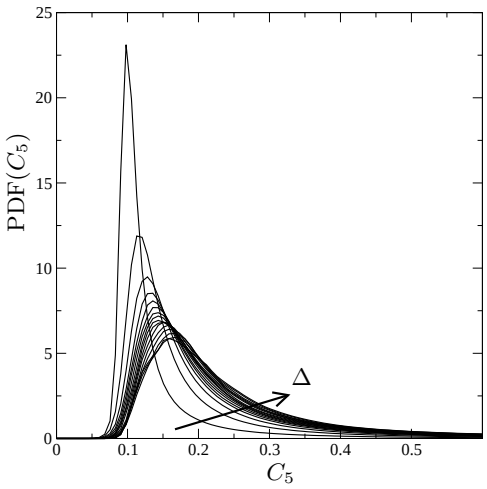

FIGURE 8. PDF of C_5 (Eq. 3.24) for several filter sizes. The arrow indicates the filter size increasing.

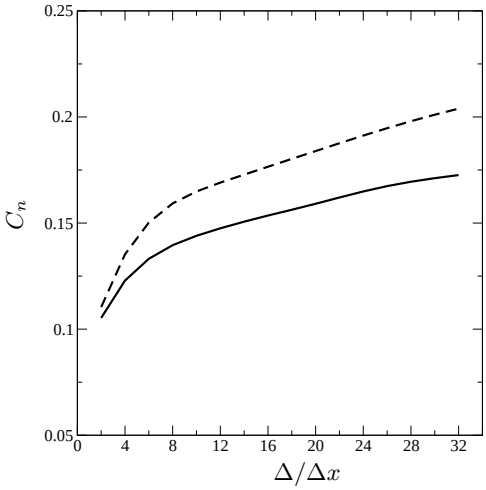

FIGURE 9. Model constant computing following both ways given in Eqs. 3.25 and 3.26. $C_n = \langle L_n M_n \rangle / \langle M_n M_n \rangle$ ——— ; $C_n = \langle L_n \rangle / \langle M_n \rangle$ - - - - .

formulation can be written as

$$z_{v,NM} = C_n \Delta^2 \frac{\partial \bar{z}}{\partial x_i} \frac{\partial \bar{z}}{\partial x_i}. \tag{3.22}$$

Since the Leonard term, $\widetilde{\bar{z}\bar{z}} - \tilde{\bar{z}}\tilde{\bar{z}}$, is available in LES, the Taylor series expansion of this term can be used to determine the dynamic coefficient. The expansion 3.19 is written for the test filter with $f = \bar{z}$ and $g = \bar{z}$. This leads to

$$\widetilde{\bar{z}\bar{z}} - \tilde{\bar{z}}\tilde{\bar{z}} = \frac{\tilde{\Delta}^2}{12} \frac{\partial \tilde{\bar{z}}}{\partial x_i} \frac{\partial \tilde{\bar{z}}}{\partial x_i} + \frac{\tilde{\Delta}^4}{288} \frac{\partial^2 \tilde{\bar{z}}}{\partial x_i \partial x_j} \frac{\partial^2 \tilde{\bar{z}}}{\partial x_i \partial x_j} + \dots . \tag{3.23}$$

Equation 3.23 shows that $\widetilde{\bar{z}\bar{z}} - \tilde{\bar{z}}\tilde{\bar{z}}$ can be evaluated from the derivatives of $\tilde{\bar{z}}$, which are also available in LES. Here, we keep only the first-order term of the RHS, and introduce a dynamic coefficient to account for the truncation error. This coefficient is assumed to be equal to C_n, already used in Eq. 3.22.

To assess this assumption, a spatially dependent quantity C_5 is defined as

$$\widetilde{\bar{z}\bar{z}} - \tilde{\bar{z}}\tilde{\bar{z}} = C_5 \tilde{\Delta}^2 \frac{\partial \tilde{\bar{z}}}{\partial x_i} \frac{\partial \tilde{\bar{z}}}{\partial x_i}. \tag{3.24}$$

The PDFs of C_5 for several filter sizes are shown in Fig. 8. The distribution of C_5 is uni-modal with a distinct peak as already seen with C_1. Moreover, the range of values of C_5 is close to the range of values of C_1. This confirms that the assumptions that C_1 and C_5 are constant over homogeneous directions and that $C_1 = C_5 = C_n$ are valid. Assuming that C_n is constant over homogeneous directions, a simple average yields

$$C_n = \frac{\langle L_n \rangle}{\langle M_n \rangle}, \tag{3.25}$$

with $L_n = \widetilde{\bar{z}\bar{z}} - \tilde{\bar{z}}\tilde{\bar{z}}$ and $M_n = \tilde{\Delta}^2 \frac{\partial \tilde{\bar{z}}}{\partial x_i} \frac{\partial \tilde{\bar{z}}}{\partial x_i}$. Instead, C_n can also be evaluated from a

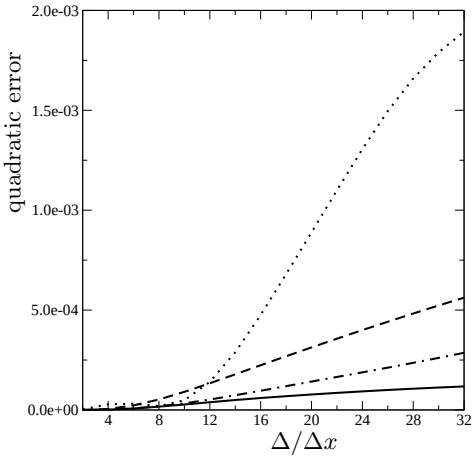

FIGURE 10. Evolution of the quadratic errors of the models $z_{v,DM}$, $z_{v,o2}$ and $z_{v,NM}$ and the associated irreducible error with the filter width. $\langle (z_v - \langle z_v|\phi_1\rangle)^2\rangle$ ——— ; $\langle (z_v - z_{v,DM})^2\rangle$ ····· ; $\langle (z_v - z_{v,o2})^2\rangle$ - - - - ; $\langle (z_v - z_{v,NM})^2\rangle$ —·— .

least-squares approximation according to Lilly's method (Lilly 1992) as

$$C_n = \frac{\langle L_n M_n\rangle}{\langle M_n M_n\rangle}. \tag{3.26}$$

Figure 9 shows that both methods are close. In the following, C_n is computed with least-squares averaging.

3.2.3. A priori *tests of new model*

The expansion 3.19 is given assuming a Gaussian filter. Hence the question of validity of the expansion 3.19 for the box filter is important, even though it is known that results are practically independent of the filter type when the box or the Gaussian filters are used (Borue & Orszag 1998; Liu *et al.* 1994). Therefore, the box filter is used in the context of the *a priori* tests presented in the following.

Figure 10 shows the quadratic errors for the different models. Note that the model $z_{v,o2}$ given by Eq. 3.21 is also tested for comparison. For all filter sizes, the quadratic error of $z_{v,NM}$ is smaller than the quadratic errors obtained with the two other models. Moreover, the quadratic error of the new dynamic procedure stays close to the irreducible error, whereas the quadratic error of the dynamic Smagorinsky-type model increases strongly. This shows that $z_{v,NM}$ is close to the best possible model using only ϕ_1 as variable set. Note also that the quadratic error of $z_{v,NM}$ is very close to the irreducible error using ϕ_2 as a set of quantities (see Fig. 3). This shows that $z_{v,NM}$ will be more accurate than a scale-similarity model independently of the scale-similarity constant C_s.

To assess the quality of a model, a scatter plot showing the model result, $g(\phi)$, versus the modeled quantity, z_v, is often used. In the same spirit, Moreau *et al.* (2006) proposed to consider $\langle z_v|g(\phi)\rangle$ as a function of $g(\phi)$. They demonstrate that the model is optimal when $\langle z_v|g(\phi)\rangle = g(\phi)$. Figure 11 shows $\langle z_v|z_{v,model}\rangle$ as function of $f(z_{v,model})$ for $\Delta/\Delta x = 14$. The figure shows that both models $z_{v,DM}$ and $z_{v,o2}$ lead to an under-prediction of the subfilter scalar variance. For the dynamic Smagorinsky-type model, the under-prediction is due to the large part of negative values of C_4 as previously observed. For $z_{v,o2}$, the under-prediction is due to the truncation error, since all the terms of the ex-

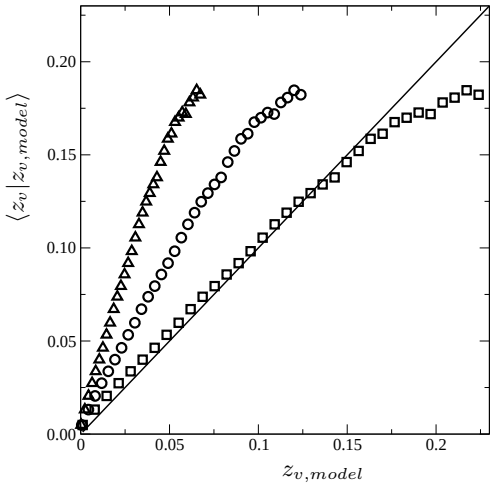

FIGURE 11. Plot of $\langle z_v | z_{v,model} \rangle = f(z_{v,model})$ for $\Delta/\Delta x = 14$; $z_{v,DM}$ △ △ △ ; $z_{v,o2}$ ○ ○ ○ ; $z_{v,NM}$ □ □ □ ; $y = x$ ——— .

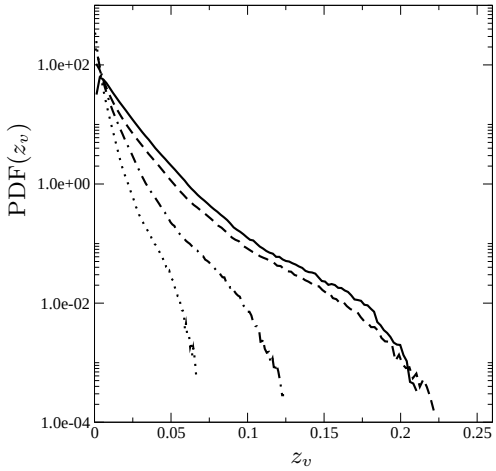

FIGURE 12. PDF of the subfilter scalar variance for $\Delta/\Delta x = 14$. z_v ——— ; $z_{v,DM}$ ····· ; $z_{v,o2}$ —·— ; $z_{v,NM}$ – – – – .

pansion 3.19 are positive. For the new dynamic model, there is just a weak over-prediction of the high values of the subfilter scalar variance, but for most of the range of the scalar variance, the model is in excellent agreement with the data. Finally, Fig. 12 shows the probability density functions of the subfilter scalar variance predicted by each model for $\Delta/\Delta x = 14$. The models are compared with the subfilter scalar variance, z_v, evaluated from the filtered DNS. As expected, the agreement between the new dynamic procedure, $z_{v,NM}$, and the filtered DNS data is very good, whereas the other models under-predict the DNS data substantially.

4. Conclusions

The dynamic variance model by Pierce & Moin (1998) was evaluated using the concept of optimal estimators. It was found that the main assumptions used in the model formulation leads to large errors in the variance predictions. The dynamic model assumes the same model coefficient can be applied at both filter levels. Moreover it is assumed that the application of the test filter is equivalent to first applying the regular filter followed by test-filtering. A Taylor-expansion analysis shows that this assumption is equivalent to neglecting a first-order term in the expansion $\widetilde{\overline{z}\overline{z}} - \widetilde{\overline{z}}\widetilde{\overline{z}}$. Inclusion of higher-order expansion terms led to a new dynamic model formulation. *A priori* tests using DNS of homogeneous isotropic turbulence showed that the new model substantially increase predictive accuracy. As part of our ongoing work, this new model is being tested in inhomogeneous flows. Further, the models developed here are being extended to describe the subfilter scalar dissipation rate, which is yet another important parameter used in describing turbulent combustion.

5. Acknowledgments

The authors gratefully acknowledge funding from NASA.

REFERENCES

Alvelius, K. 1999 Random forcing of three-dimensional homogeneous turbulence. *Phys. Fluids* **11**, 1880–1889.

Bedford, K. W. & Yeo, W. K. 1993 Conjective filtering procedures in surface water flow and transport. *Large Eddy Simulation of Complex Engineering and Geophysical Flows*, edited by B. Galperin and S. A. Orszag. New York: Cambridge University Press.

Borue, V. & Orszag, S. 1998 Local energy flux and subgrid-scale statistics in three-dimensional turbulence. *J. Fluid Mech.* **366**, 1–31.

Clark, R. A., Ferziger, J. H. & Reynolds, W. C. 1979 Evaluation of subgrid-scale models using an accurately simulated turbulent flow. *J. Fluid Mech.* **91**, 1–16.

Cook, A. W. & Riley, J. J. 1994 A subgrid model for equilibrium chemistry in turbulent flows. *Phys. Fluids* **6**, 2868–2870.

Donzis, D. A., Sreenivasan, K. R. & Yeung, P. K. 2005 Scalar dissipation rate and dissipative anomaly in isotropic turbulence. *J. Fluid Mech.* **532**, 199–216.

Jimenez, J. & Wray, A. A. 1998 On the characteristics of vortex filaments in isotropic turbulence. *J. Fluid Mech.* **373**, 255–285.

Lesieur, M. & Métais, O. 1996 New trends in large-eddy simulations of turbulence. *Ann. Rev. Fluid Mech.* **28**, 45–82.

Lilly, D. K. 1992 A proposed modification of the Germano subgrid-scale closure method. *Phys. Fluids A* **4**, 633–635.

Liu, S., Meneveau, C. & Katz, J. 1994 On the properties of similarity subgrid-scale models as deduced from measurements in a turbulent jet. *J. Fluid Mech.* **275**, 83–119.

Meneveau, C. & Katz, J. 1996 Scale-invariance and turbulence models for large-eddy simulation. *Ann. Rev. Fluid Mech.* **28**, 45–82.

Meneveau, C., Lund, T. S. & Cabot, W. 1996 A Lagrangian dynamic subgrid-scale model of turbulence. *J. Fluid Mech.* **319**, 353–386.

Moreau, A., Teytaud, O. & Bertoglio, J. P. 2006 Optimal estimation for large-eddy simulation of turbulence and application to the analysis of subgrid models. *Phys. Fluids* **18**, 1–10.

Pope, S. B. 2000 *Turbulent Flows*. New-York: Cambridge University Press.

Pierce, C. D. & Moin, P. 1998 A dynamic model for subgrid-scale variance and dissipation rate of a conserved scalar. *Phys. Fluids* **10**, 3041–3044.

Pitsch, H. 2006 Large-eddy simulation of turbulent combustion. *Ann. Rev. Fluid Mech.* **38**, 453–482.

Pomraning, E. & Rutland, C. J. 2002 Dynamic one-equation nonviscosity large-eddy simulation model. *AIAA Journal* **40**, 689–701.

Rogallo, R. S. & Moin, P. 1984 Numerical simulation of turbulent flows. *Ann. Rev. Fluid Mech.* **16**, 99–137.

da Silva, C. B. & Pereira, J. C. F. 2007 Analysis of the gradient-diffusion hypothesis in large-eddy simulations based on transport equations. *Phys. Fluids* **19**, 1–20.

Wall, C., Boersma, B. J. & Moin, P. 2000 An evaluation of the assumed beta probability density function subgrid-scale model for large eddy simulation of nonpremixed, turbulent combustion with heat release. *Phys. Fluids* **12**, 2522–2529.